Interference Modeling in CSMA Multi-Hop Wireless Networks

Anthony Busson, Guillaume Chelius, Jean-Marie Gorce

INSTITUT NATIONAL DE RECHERCHE EN INFORMATIQUE ET EN AUTOMATIQUE

Interference Modeling in CSMA Multi-Hop Wireless Networks

Anthony Busson — Guillaume Chelius — Jean-Marie Gorce

N° 6624

February 2009

Thème COM

ISSN 0249-6399 ISRN INRIA/RR--6624--FR+ENG

INSTITUT NATIONAL
DE RECHERCHE
EN INFORMATIQUE
ET EN AUTOMATIQUE

INRIA

centre de recherche
GRENOBLE - RHÔNE-ALPES

Interference Modeling in CSMA Multi-Hop Wireless Networks

Anthony Busson* , Guillaume Chelius† , Jean-Marie Gorce‡

Thème COM — Systèmes communicants
Équipes-Projets A4RES

Rapport de recherche n° 6624 — February 2009 — 18 pages

Abstract: In analytical studies of multi-hop wireless networks, the spatial distribution of transmitters is typically modeled using a homogeneous Poisson point process. In this report, we show why such a modeling is inaccurate and leads to an inappropriate interference distribution in the case of CSMA/CA networks. We then study a more realistic model, the Matèrn point process, which still reveals some unexpected flaws such as an under-estimation of the transmitters density. To get round these limitations, we propose the use of an alternate model, referred to as the *Simple Sequential Inhibition* (SSI) point process, which we assert being a valuable and more appropriate model for CSMA/CA networks. We present some analytical results on the Matèrn and the SSI model and study by simulation the interference distribution resulting from the different point processes.

Key-words: interference modeling, stochastic geometry, multi-hop wireless networks, SSI point process, Matèrn point process

* IEF - CNRS, 91405 Orsay, France - anthony.busson@u-psud.fr
† University of Lyon, INRIA ENS Lyon, F-69364, France - guillaume.chelius@inria.fr
‡ University of Lyon, INSA-Lyon, INRIA, F-69621, France - jean-marie.gorce@insa-lyon.fr

Centre de recherche INRIA Grenoble – Rhône-Alpes
655, avenue de l'Europe, 38334 Montbonnot Saint Ismier
Téléphone : +33 4 76 61 52 00 — Télécopie +33 4 76 61 52 52

Modelisation des interférences dans les réseaux sans-fil multi-sauts

Résumé : Dans les études analytiques concernant les réseaux sans-fil multi-sauts, la distribution spatiale des émetteurs est généralement modélisée par un processus ponctuel de Poisson. Dans ce rapport, nous décrivons les limites de ce modèle et leurs conséquences sur la distribution du niveau d'interférence dans des réseaux de type CSMA/CA. Nous étudions ensuite un modèle plus réaliste, le processus ponctuel de Matèrn, qui présente également un certains nombres de défauts conduisant à une sous-évaluation de l'intensité des interférants. Afin de contourner ces limitations, nous proposons finalement l'utilisation d'un troisième modèle, appelé processus ponctuel SSI (*Simple Sequential Inhibition*), que nous affirmons être d'avantage approprié dans le contexte des réseaux CSMA/CA. Nous présentons dans ce rapport quelques résultats analytiques liés aux modèles SSI et Matèrn et étudions la distribution des interférences générées par ces deux processus ponctuels.

Mots-clés : modélisation des interférences, géométrie stochastique, réseaux sans-fil multi-sauts, processus ponctuel SSI, processus ponctuel Matèrn

1 Introduction

Multi-hop radio networks have been analytically studied for more than 20 years. Some fundamental results have been obtained concerning the capacity and the connectivity of the network [9, 8] but at the price of strong assumptions about the physical layer. More recent works have addressed the performance evaluation of multi-hop radio networks under more realistic constraints. A first trend consists in improving the realism of the radio channel, including phenomenon such as radiation patterns, fading and shadowing. As a deterministic study requires the knowledge of a specific environment, these phenomena are generally considered from a statistical point of view [2, 11, 16, 17].

Taking into account interference is a second way to improve the realism of multi-hop networks modeling. Several works have introduced interference [11, 20] by modeling the overall interference power as a statistical variable including the contribution of all simultaneous transmitters. In most of these approaches, the lack of knowledge about the transmitter positions have lead authors to consider the spatial distribution of the transmitters as Poisson distributed. This assumes that their positions are not correlated. Under complementary assumptions about the fading strength, this approach leads to an analytical expression of the interference distribution [1].

In this research report, we point out the main limitations of this model. Indeed, most of wireless networks exploit a resource sharing strategy, which means that the existence of two interferers in their vicinity is not possible. Concerning CSMA/CA-like networks, it has been earlier advocated that the use of a Matèrn point process [1] leads to a more realistic model as it introduces an exclusion area around nodes. In Section 3, we present some analytical results on the Matèrn. In particular, we give the mean and variance of interference resulting from Matèrn distributed emitters, and the proportion of the plane covered by the inhibition balls of the Matérn. All these results are, to our knowledge, new. Albeit, we show that this model suffers from some unexpected properties, such as an underestimation of concomitant active transmitters. To get round these limitations, we propose in section 4 the use of an alternate model referred to as the *Simple Sequential Inhibition* (SSI) point process, which we assert being a valuable and more appropriate model for CSMA/CA networks. In Section 5, we compare the interference distribution resulting from the different point processes and show that they offer very different behavior. We finally conclude in Section 6.

2 Physical layer modeling

2.1 Propagation modeling

At a given location x_j ($x_j \in I\!R^2$), the power of a signal received from node x_i is given by $S_i \cdot h_{ij}$ where h_{ij} is the path-loss over (x_i, x_j) , and S_i the transmission power of x_i. The path-loss function depends on the propagation model. In most cases, one have $h_{ij} = l(\|x_j - x_i\|)$ where $\|.\|$ is the Euclidean norm in $I\!R^2$ and $l(.)$ is a decreasing function from $I\!R^+$ in $I\!R^+$, standing for the power decay with respect to the distance.

In the following, our results are valid for any bounded continuous decreasing function $l(.)$ and numerical simulations are obtained using an adapted Friis Formula, $l(u) = min(1, \left(\frac{\mu}{4\pi u}\right)^{\alpha})$ where α is a parametric path-loss exponent typically ranging from 2.0 to 6.0 and μ is the radio signal carrier wavelength.

2.2 Interference modeling

As mentioned before, interference plays a fundamental role in the capacity of wireless networks. When a single channel is used for several nodes, interference is referred to as co-channel interference. It is usual to consider the overall interference as a corruptive noise which affects the reception quality. In this case, the interference strength is equal to the sum of the interfering signals:

$$I_{\Phi}(x_j, t) \quad = \quad \sum_{x_i \in \Phi} S_i \cdot l(\|x_j - x_i\|) \cdot \mathbf{s}_{ij} \cdot \mathbf{f}_{ij}(t) \tag{1}$$

where Φ is the set of interfering nodes.

The use of this equation is valid only for linear receivers and only if the interference behaves roughly like the receiver noise. This assumption may fail if the number of interferers is low or if it exists one or few interfering signals having a largely higher power than the others. In this case, the strong interferers produce a correlated noise which affects in depth the performance of the receiver. In many applications, this problem doesn't hold because a *Medium Access Control* (MAC) policy is used to prevent near interferers.

3 Modeling of CSMA-CA networks: the Matèrn point process

In analytical studies of multi-hop wireless networks [1, 5, 6], the location of emitters is typically modeled using a homogeneous Poisson point process. With a Poisson point process, the transmitter locations are assumed independent. This strong assumption is not valid in most of wireless multi-hop networks. The use of a *Medium Access Control* (MAC) protocol generally ensures that two close nodes do not emit simultaneously, either by assigning them different frequency (FDMA) or time (TDMA) resources or by implementing a CSMA/CA mechanism.

In a CSMA/CA network, a potential transmitter senses the channel before effectively transmitting. Depending on whether the channel is assessed clear or not, the transmission occurs or is postponed. *Clear Channel Assessment* (CCA) depends on the MAC protocol and the terminal settings. For the two most widely used CSMA/CA protocols, IEEE 802.11 DCF and IEEE 802.15.4, CCA is performed according to one of these three methods. (*mode 1*) CCA reports a busy medium upon detecting any energy above the Energy Detection threshold. (*mode 2*) CCA shall report a busy medium only upon the detection of a compliant signal. (*mode 3*) CCA reports a busy medium using a *OR* or *AND* logical combination of the two previous conditions.

A direct consequence of CSMA/CA is that transmitters cannot be very closed to each others. The Poisson point process does not take into account this constraint and leads to a large inaccuracy in the distribution of emitters for a CSMA/CA network. This results in an inappropriate interference distribution as it will be shown in Section 5.

3.1 The Matèrn point process

An alternate point process has been advocated in [3, 1] to model the location of transmitters in a CSMA/CA network and studied in [18] to model dense IEEE 802.11 networks: the Matèrn point process [15]. A Matèrn point process is a particular thinning of a homogeneous Poisson point process Φ such that the distance between two selected nodes is always greater than r, $r > 0$. In our context, the Poisson point process represents the potential transmitters whereas the Matèrn point process models the effective ones.

Here, we consider an alternate temporal version of the Matèrn point process. Our process $\Phi_M(n)$ is build in a finite observation window $B(O, R)$ rather than in the plane. We consider a sequence of random variables $(X_i)_{i=1,..,n}$ independently and uniformly distributed in a ball of radius R, denoted B. The point X_1 is distributed first and systematically selected in $\Phi_M(1)$. At the i^{th} step, the point X_i is distributed and selected in $\Phi_M(i)$ if and only if none of the $i-1$ previous points lies in B_{X_i}, the ball centered at X_i with radius r, r being an exclusion range. The procedure stops when the n points have been considered. Note that if n follows a discrete Poisson law, we get the classical Matèrn point process restricted to B. The temporal sequence of the alternate Matèrn is then equivalent to the mark sequence of the classical Matèrn. Section 3.3 presents some theoretical results on this temporal Matèrn point process.

Thanks to its particular selection process, the Matèrn point process seems well-suited to model a network operating in CCA *mode 2*. Indeed, a transmitter postpones its emission upon detection of a compliant signal, *i.e.* the presence of a transmitter within detection distance. However, spatial considerations reveal some fundamental limitations.

3.2 Spatial limitations

The main flaw of the Matèrn point process lies in its selection process. A point of the original point process Φ which has not been selected in the Matèrn $\Phi_M(n)$ inhibits nevertheless all the nodes with a lower mark within its exclusion ball. For instance, let us consider the scenario in Figure 1. Nodes 1 and 4 are legitimately selected as transmitters. Node 2 is not selected as it is within the exclusion ball of node 1. Node 3 is not selected as its mark is less than the one of node 2 despite the fact that node 2 is not selected. In the CSMA/CA perspective, this is inexact as only effective transmitters inhibit potential ones.

The fact that unselected points play a role in the selection process limits the emitters coverage to a portion of the plane. Indeed, when the intensity of the underlying point process Φ tends to infinity, the union of the exclusion balls associated to the selected points covers only approximately 78% of the plane (see Section 3.3). A large part of potential transmitters which would be selected in reality is not considered in the Matèrn point process. The direct consequence is an underestimation of the effective transmitters intensity in the network and so far an underestimation of the interference level when compared to the reality.

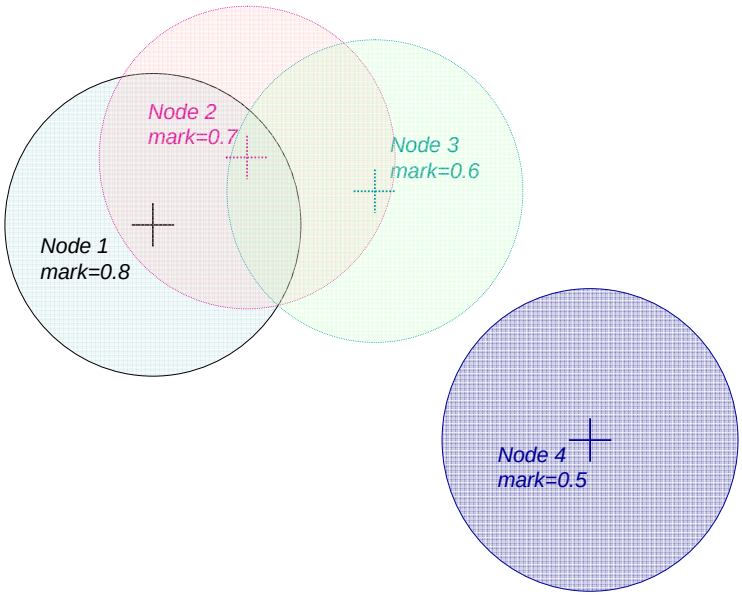

Figure 1: The Matèrn selection process

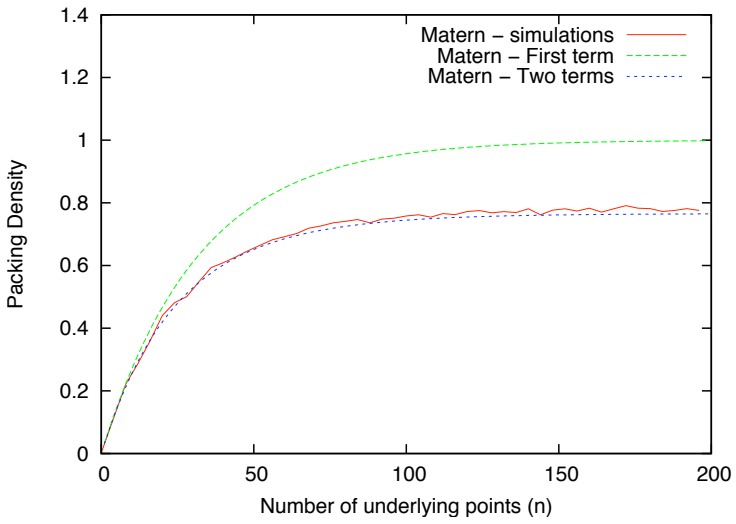

Figure 2: The Matèrn packing density.

3.3 Intensity, spatial distribution and coverage

We present here different results on the alternate Matèrn point process. The first one is simply the mean number of nodes in the observation area and its asymptotic behavior when R tends to infinity. A Proposition then gives the spatial distribution of k nodes randomly chosen among the points of $\Phi_M(n)$. The last Proposition presents a result on the mean plane coverage induced by the Matèrn exclusion balls. In the next Section, we present the mean and variance of interference generated by emitters distributed according to the alternate Matèrn point process. The proofs can be found in Appendix 7.

Let $N_M(n)$ be the random variable describing the number of points in $\Phi_M(n) \cap B$, we get:

$$\begin{aligned}\mathbb{E}\left[N_M(n)\right] &= \sum_{i=1}^{n} \mathbb{P}\left(X_i \in \Phi_M(n)\right) \\ &= \sum_{i=1}^{n} \frac{(R-r)^2}{R^2}\left(1-\frac{\pi r^2}{\pi R^2}\right)^{i-1} + \int_{R-r}^{R} f(u)\left(\frac{A(u,r,R)-\pi r^2}{\pi R^2}\right)^{i-1} du \\ &= \frac{(R-r)^2}{R^2}\frac{R^2}{r^2}\left[1-\left(1-\frac{r^2}{R^2}\right)^n\right] + \int_{R-r}^{R} 2\pi u \frac{1-\left(\frac{A(u,r,R)-\pi r^2}{\pi R^2}\right)^n}{\pi R^2 - A(u,r,R) + \pi r^2} du \end{aligned} \quad (2)$$

where $A(u,r,R)$ denotes the area of the union of two discs of radius r and R with their centers at distance u.

$$A(u,r,R) = ur\sqrt{1-\left(\frac{1}{2}\frac{r^2+u^2-R^2}{ur}\right)^2} + u^2 \arccos\left(-\frac{1}{2}\frac{r^2+u^2-R^2}{Rr}\right) + R^2 \arccos\left(-\frac{1}{2}\frac{r^2-u^2+R^2}{Rr}\right)$$

if $u < r+R$ and $A(u,r,R) = \pi r^2 + \pi R^2$ if $u \geq r+R$.

If $R \to +\infty$ and $n \sim \lambda \pi R^2$,

$$\lim_{R\to+\infty} \frac{\mathbb{E}\left[N_M(n)\right]}{\pi R^2} = \frac{1-e^{-\lambda\pi r^2}}{\pi r^2}$$

Proposition 1. *Let $\Phi_M(n)$ be the modified Matèrn point process distributed in B, $(X_{i_1},..,X_{i_k})$ a subset of points of the original sequence $(X_i)_{i=1,..,n}$ with $1 \leq i_1 < i_2 < .. < i_k \leq n$, $kr^2 < R^2$ and $A_1,..,A_n$ a set of Borel sets of $\mathbb{R}^2$ such that $A_i \subset B\ \forall i = 1,..,k$, we get*

$$\begin{aligned}&\mathbb{P}\left(X_{i_j} \in A_j \forall j \in \{1,..,k\}, X_{i_j} \in \Phi_M(n) \forall j \in \{1,..,k\}\right) = \\ &\left(\frac{1}{\pi R^2}\right)^k \int_{A_1}\int_{A_2\setminus B_{x_1}}\int_{A_3\setminus B_{x_1}\cup B_{x_2}} \cdots \int_{A_k\setminus\left(\bigcup_{j=1}^{k-1} B_{x_j}\right)} \prod_{j=1}^{k} \nu\left(B\setminus\bigcup_{v=j}^{k-1} B_{x_v}\right)^{i_j-i_{j-1}-1} dx_k...dx_1 \end{aligned} \quad (3)$$

For $k=1$, we get

$$\mathbb{P}\left(X_{i_1} \in A_1, X_{i_1} \in \Phi_M(n)\right) = \frac{1}{\pi R^2}\int_{A_1}\left(\frac{\nu\left(B\setminus B_{x_1}\right)}{\pi R^2}\right)^{i_1-1} dx_1 \quad (4)$$

In the next Proposition, we compute the mean area covered by the union of balls B_{X_i}. Let $\Xi_M(n)$ be the random closed set defined as:

$$\Xi_M(n) = \bigcup_{X_i \in \Phi_M(n)} B_{X_i} \cap B$$

We define the *packing density* as $\frac{\mathbb{E}[\Xi_M(n)]}{\pi R^2}$.

Proposition 2. *If $n \sim \lambda\pi R^2$ with $\lambda \in \mathbb{R}^+$, we get*

$$\lim_{R\to+\infty} \frac{\mathbb{E}\left[\Xi_M(n)\right]}{\pi R^2} = (1-e^{-\lambda\pi r^2}) - \frac{1}{\pi r^2}\int_{B(O,2r))\setminus B_O} \nu(B_O\cap B_y)\Big(\frac{1-e^{-\lambda\nu(B_O\cup B_y)}}{\nu(B_O\cup B_y)} - \frac{e^{-\lambda\pi r^2}-e^{-\lambda\nu(B_O\cup B_y)}}{\nu(B_O\cup B_y)-\pi r^2}\Big)dy + K_3(\lambda,r) - K_4(\lambda,r) + K_5(\lambda,r) \quad (5)$$

The addition $\oplus$ is the Minkowski-addition. The three functions $K_3(\lambda,r)$, $K_4(\lambda,r)$ and $K_5(\lambda,r)$ are detailed in Appendix 7.1.

Note that for the numerical evaluation, as shown in Figure 2, the two first quantities of equation 5 are sufficient to obtain very a accurate estimation of the packing density. It is the reason why we do not specify here the formulae for the quantity $K_3(.)$, $K_4(.)$ and $K_5(.)$. We also observe that when λ tends to infinity, the packing density converges to ≈ 0.78.

3.4 Mean and variance of interference for the alternate Matèrn point process

In this Section we compute the mean and variance for the interference generated by emitters distributed according to the alternate Matèrn point process. The level of interference is computed at the center of the observation window B, denoted O.

3.5 Interference from Matèrn distributed emitters

From the distribution of a point in the Matèrn point process, we can easily deduce the mean interference level at O, according to the following Proposition.

Proposition 3.

$$\mathbb{E}\left[I_{\Phi_M(n)}(O)\right] = 2\pi\int_0^R u\frac{1-\left(\frac{A(u,r,R)-\pi r^2}{\pi R^2}\right)^n}{\pi R^2+\pi r^2-A(u,r,R)}l(u)du$$

If n is constant and R tends to infinity, $\mathbb{E}[I_{\Phi_M(n)}(O)]$ tends to 0. If $n\sim\lambda\pi R^2$,

$$\lim_{R\to+\infty}\mathbb{E}\left[I_{\Phi_M(\lambda\pi R^2)}(O)\right] = \frac{1-e^{-\lambda\pi r^2}}{\pi r^2}\int_{\mathbb{R}^2} l\left(\|x\|\right)dx$$

For the special attenuation function $l(u)=min(1,u^{-\alpha})$ with $\alpha>2$, we have

$$\lim_{R\to+\infty}\mathbb{E}\left[I_{\Phi_M(\lambda\pi R^2)}(O)\right] = 2\frac{1-e^{-\lambda\pi r^2}}{r^2}\left(\frac{1}{2}+\frac{1}{\alpha-2}\right)$$

For the second moment:

$$\mathbb{E}\left[I^2_{\Phi_M(n)}(O)\right] = \int_B \frac{1-\left(\frac{\nu(B\setminus B_x)}{\pi R^2}\right)^n}{\pi R^2-\nu(B\setminus B_x)}l\left(\|x\|\right)^2dx + 2\int_B\int_{B\setminus B_x}\frac{1}{\pi R^2-\nu(B\setminus B_x\cup B_y)}\Big[\frac{1-\left(\frac{\nu(B\setminus B_x\cup B_y)}{\pi R^2}\right)^{n-1}}{\pi R^2-\nu(B\setminus B_x\cup B_y)} - \frac{\left(\frac{\nu(B\setminus B_y)}{\pi R^2}\right)^{n-1}-\left(\frac{\nu(B\setminus B_x\cup B_y)}{\pi R^2}\right)^{n-1}}{\pi R^2\left(1-\frac{\nu(B\setminus B_x\cup B_y)}{\nu(B\setminus B_y)}\right)}\Big]dydx \quad (6)$$

When $R\to+\infty$ and $n\sim\lambda\pi R^2$,

$$\lim_{R\to+\infty} \mathbb{E}\left[I^2_{\Phi_M(n)}(O)\right] = \frac{1-e^{-\lambda\pi R^2}}{\pi r^2}\int_{\mathbb{R}^2} l\left(\|x\|\right)^2 dx + \frac{2}{\pi r^2}\int_{\mathbb{R}^2}\int_{\mathbb{R}^2\setminus B_x}\left[\frac{1-e^{-\lambda\nu(B_x\cup B_y)}}{\nu(B_x\cup B_y)} - \frac{e^{-\lambda\pi r^2}-e^{-\lambda\nu(B_x\cup B_y)}}{\nu(B_x\cup B_y)-\pi r^2}\right] l\left(\|x\|\right) l\left(\|y\|\right) dydx \quad (7)$$

4 Modeling of CSMA-CA networks: the SSI point process

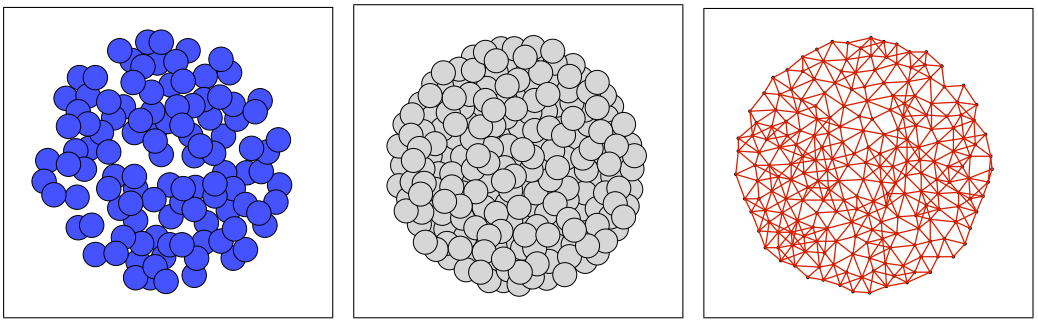

(a) A sample of a Matèrn point process.

(b) A sample of a SSI point process.

(c) Graph of SSI points after saturation ($n \to +\infty$)

Figure 3: Samples of the Matèrn and SSI point process after saturation with $R = 1$ and $r = 0.1$.

As shown in Section 3, the Matèrn point process presents several flaws regarding the modeling of transmitters in a CSMA/CA network. In this section, we discuss another point process, the *Simple Sequential Inhibition* (SSI) point process, as being a valuable and more appropriate model for CSMA/CA networks. The SSI point process has been introduced by Palásti [19]. This model belongs to a family of well-known models used in the context of *packing problems* or *space filling*. They are concerned with the distribution of *solids* in k-dimensional spaces [10, 21]. The SSI point process is also known as the Poisson disk distribution and is used in computer graphics to efficiently sample images [4, 25].

A SSI point process, $\Phi_S(n)$, is a constructive point process distributed in a finite area of the plane, B. Let $X_1, ..., X_n$ be a sequence of random variables independently and uniformly distributed in B. X_1 is systematically added to $\Phi_S(1)$. X_i is added to $\Phi_S(i)$ if and only if $X_i \notin \cup_{X_j\in\Phi_S(i-1)} B_{X_j}$ where B_{X_j}. The process stops whenever the n points have been considered or when B is entirely covered by the union of the inhibition balls.

We shall say that a sample of the SSI has reached saturation when the union of the inhibition balls associated to the selected points covers entirely B. Note that the temporal Matèrn point process is a thinning of the SSI. The interference level generated by Matèrn distributed emitters is then a lower bound of the interference level generated by SSI distributed emitters. Figures 3(a) and 3(b) depict samples of Matèrn and SSI point processes after saturation. We can clearly see that with n large enough , the SSI covers entirely B whereas the Matèrn does not. The SSI model compensates for the main flaw of the Matèrn model as it considers only the inhibition balls associated to effective transmitters during the selection process.

Very few theoretical results exist for SSI point processes. For instance, we have no result on the mean number of points in B or the probability for a point X_i to be selected in $\Phi_S(n)$. However, some values have been approximated. The mean number of nodes in B after saturation can be approximated by $\frac{4c^2R^2}{r^2}$, where c is the *packing density*. In our case, $c = 0.56$ [14]. It has been also conjectured that the ratio $\frac{\mathbb{E}\left[\sum_{X_i\in\Phi_S}^{+\infty}\nu(B_i)\right]}{\pi R^2}$ converges to the constant $4c$. Other estimations approximate the distribution of nodes or the distance between closest points [12].

4.1 Mean and variance of interference for the SSI point process

There is no theoretical result about the distribution of $\Phi_S(n)$. However, as shown by simulations, for R large enough, the distribution of one point arbitrarily chosen among the points of $\Phi_S(n)$ can be approximated by the uniform distribution. For smaller R (for instance $R = 1.0$ and $r = 0.1$), we observe some edge effects at the boundary of B. Under this assumption, we can derive the mean interference level:

$$\begin{aligned}\mathbb{E}\left[I_{\Phi_S(n)}(O)\right] &= \sum_{i=1}^{n} \mathbb{E}\left[l(\|X_i\|)\mathbb{1}_{X_i\in\Phi_S(n)}\right] \\ &\approx \mathbb{E}\left[N_S(n)\right]\frac{2}{R^2}\int_0^R ul(u)du\end{aligned}$$

where $N_S(n)$ is the number of points in $\Phi_S(n)$. Unfortunately, $\mathbb{E}[N_S(n)]$ is not known. Nevertheless, when the process has reached saturation ($n \to +\infty$), it can be approximated by $\mathbb{E}[N_S(n)] \approx 4c\frac{R^2}{r^2}$ [14].

5 Interference with CSMA-CA protocols

802.15.4 Parameters	Numerical Values	Simulation parameters	Numerical values
Frequency	868MHz	R	100.0m
Wavelength	0.346 m	Radius of inhibition (r)	14.9m
Detection Threshold (θ)	-82dBm	Number of samples	at least $800,000$
Emission power	0dBm		

Table 1: Simulation parameters.

		Poisson		Matèrn		SSI	
		Scenario 1	Scenario 2	Scenario 1	Scenario 2	Scenario 1	Scenario 2
$n = 0.2\frac{r^2}{R^2}$	normal	$6.82e^{+04}$	$1.05e^{+04}$	$4.19e^{+05}$	$2.63e^{+05}$	$1.03e^{+05}$	$1.44e^{+05}$
	log-normal	$1.73e^{+03}$	$5.42e^{+02}$	$1.06e^{+04}$	$4.06e^{+03}$	$5.33e^{+03}$	$6.58e^{+03}$
$n = 0.7\frac{r^2}{R^2}$	normal	$3.89e^{+04}$	$1.04e^{+04}$	$1.43e^{+05}$	$3.05e^{+04}$	$1.99e^{+04}$	$2.69e^{+04}$
	log-normal	$2.07e^{+03}$	$4.86e^{+02}$	$1.02e^{+04}$	$2.10e^{+03}$	$3.88e^{+03}$	$3.95e^{+03}$
$n = 20.0\frac{r^2}{R^2}$	normal	$7.71e^{+04}$	$1.00e^{+04}$	$2.15e^{+05}$	$1.41e^{+04}$	$1.25e^{+03}$	$1.25e^{+03}$
	log-normal	$1.28e^{+03}$	$1.32e^{+03}$	$9.10e^{+03}$	$1.14e^{+03}$	$1.60e^{+03}$	$1.49e^{+03}$

Table 2: Value of the χ^2 statistics.

In this Section we study the interference level *probability density function* (pdf). We use the parameters of the IEEE 802.15.4 standard at the 868 MHz frequency. These parameters are summarized in Table 1. We compare two scenarios. For both scenario, an emitter is located at $(0, \frac{r}{2})$, where r is the inhibition ball radius, and a receiver is located at the origin. In scenario 1, we suppose that there is an inhibition ball centered at the emitter. This ball models the CCA operation done by this node before emitting. In scenario 2, we add an inhibition ball centered at the receiver. This scenario models the use of a RTS/CTS handshake. Other network nodes are distributed in the observation window B according to one of the three point processes, Poisson, Matèrn and SSI, addressed so far. We consider three different density of nodes : $n = 0.2\frac{R^2}{r^2}$, $n = 0.7\frac{R^2}{r^2}$ and $n = 20.0\frac{R^2}{r^2}$. The last density value corresponds to the saturated case. In this last case, the Poisson process density is chosen equal to the SSI one.

In Figures 4(a) to 4(i), we plot the interference pdf for the different point processes. These pdf are compared to normal and log-normal distributions with same mean and variance. For all the scenarios and point processes, a χ^2 test was performed to check wether the distributions could be extrapolated by a normal or a log-normal distributions. The null hypothesis is systematically rejected at a 5% significance level. The χ^2 statistic, shown in Table 2, is used to

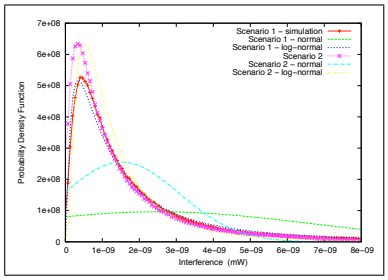

(a) Poisson. $n = 0.2\frac{R^2}{r^2}$.

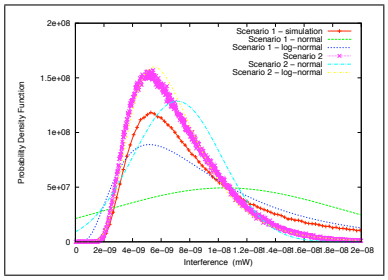

(b) Poisson. $n = 0.7\frac{R^2}{r^2}$.

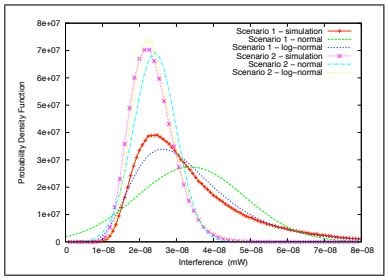

(c) Poisson. Same intensity as the SSI with $n = 20.0\frac{R^2}{r^2}$.

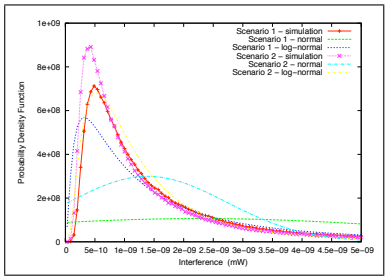

(d) Matern. $n = 0.2\frac{R^2}{r^2}$.

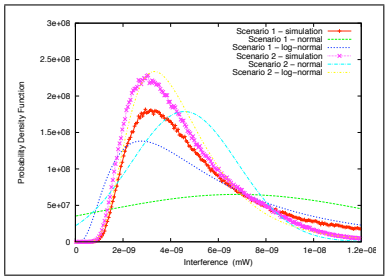

(e) Matern. $n = 0.7\frac{R^2}{r^2}$.

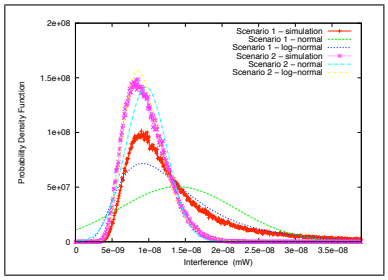

(f) Matern. $n = 20.0\frac{R^2}{r^2}$.

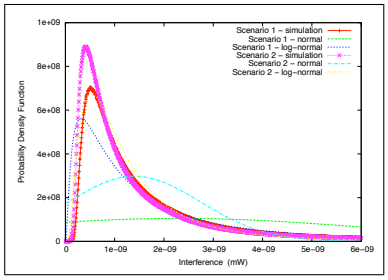

(g) SSI. $n = 0.2\frac{R^2}{r^2}$.

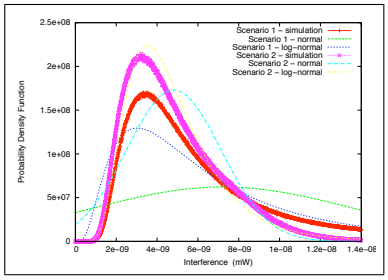

(h) SSI. $n = 0.7\frac{R^2}{r^2}$.

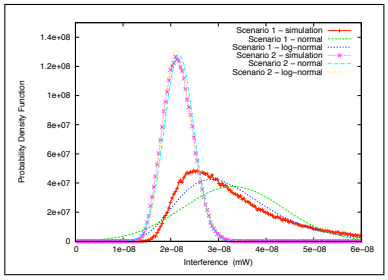

(i) SSI. $n = 20.0\frac{R^2}{r^2}$.

Figure 4: Interference Probability Density Function. Comparison between Interference, normal and log-normal distributions.

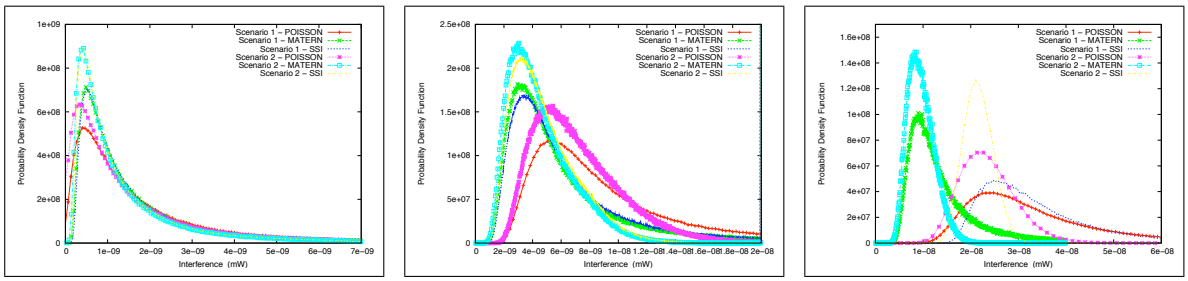

(a) $n = 0.2\frac{R^2}{r^2}$. (b) $n = 0.7\frac{R^2}{r^2}$. (c) $n = 20.0\frac{R^2}{r^2}$.

Figure 5: Interference Probability Density Function. Comparison between the different point processes.

compare the fitness of these two distributions with the empirical ones. In order to get comparable quantities, we get the same number of bins (10), and the same number of samples $(200,000)$ for all the scenarios and point processes.

With a Poisson point process, the interference distribution presents a peak and a heavy-tail. The distribution is strongly asymmetric and far from being Gaussian. This observation confirms the results of [24, 13, 7], where an heavy-tailed interference distribution is observed for Poisson distributed interferers. This observation contradicts a classical assumption in the signal processing community where the interference is generally considered to be Gaussian [23]. Several distributions such as K-distribution, Weilbull, logNormal or Laplacian distributions have been proposed to model or extrapolate this heavy-tailed distribution. More recently, the alpha-stable distributions have also been proposed [13].

With a high density of nodes and for scenario 2, the interference distribution gets however close to a normal distribution. This is due to the high intensity of emitters which garantee a certain coverage of the whole observation window. This high intensity is the result of a very small inhibition radius ($r = 14.9$ meters).

For a small intensity, the Matèrn and SSI point processes offer a similar interference distribution to the Poisson generated one (Figures 5(a) and 5(b)). As we consider a small number of potential emitters, most of them are selected as effective emitters and almost independently of each others. For $n = 0.7\frac{R^2}{r^2}$, the interference level induced by Poisson emitters gets higher in average than the ones induced by Matèrn and SSI emitters, as some potential emitters are not selected by the Matèrn and the SSI processes. But the shapes of the distributions remain comparable. We also observe in Figures 4(d), 4(e), 4(g) and 4(h), that for these two intensities, neither normal nor log-normal distributions fit the interference distribution. The log-normal law can however offer a good approximation of these pdf.

For the saturated density in scenario 2, we can see in Figures 4(f) and 4(i) that the log-normal distribution fits very well. For the SSI, the normal distribution fits as well. In Figure 5(c), we compare the interference pdf generated by the three point processes. Even if the mean interference of the SSI and Poisson processes are equal, the variance is approximately 5 times greater for the Poisson process. The Matèrn leads to a lower level of interference as it selects a smaller number of emitters.

5.1 Simulations analysis

5.1.1 Extrapolation

For small intensities ($n = 0.2\frac{R^2}{r^2}$), the log-normal distribution only offers a rough approximation of the Matèrn and SSI interference distributions. For greater intensities ($n = 0.7\frac{R^2}{r^2}$), the log-normal distribution fits well the interference distributions generated by the three point processes in scenario 2, but can only be used as an approximation in scenario 1. In the saturated case, *i.e.* dense networks, the log-normal distribution just offers an approximation for scenario 1, whereas it fits perfectly well in scenario 2. For SSI generated interference, the normal distribution matches as well and the χ^2 statistic even indicates that it is closer than the log-normal distribution.

5.1.2 Process comparisons

For small intensities ($n = 0.2\frac{R^2}{r^2}$), interference distributions generated by the SSI and the Matèrn point processes are similar. The Poisson generated interference distribution differs, its variance being greater due to a heavier distribution tail. For higher intensities ($n = 0.7\frac{R^2}{r^2}$), the SSI and Matèrn distributions start to differ, and the Poisson distribution becomes far from the two other ones. In the dense case, there is a significant difference between the mean values of the Matèrn and the SSI interference distributions. Even if, by assumptions, the means are the same for the SSI and the Poisson and both seem to be normally distributed, there is a huge difference regarding the variance of the distributions.

It is also worth noting that the Matèrn and the SSI lead to a realistic intensity of effective emitters with respect to the intensity of the potential emitters. For the Poisson case, there is no bound on the intensity.

So, except for very sparse networks, for which the interference distributions generated by the three point processes are comparable, the different point processes lead to very different interference pdf. It is obvious that these differences have a major impact on the resulting radio medium properties (Bit Error Rate, *etc*.).

6 Conclusion and perspectives

In this research report, we have discoursed about the modeling of interference in multi-hop wireless networks. We have presented the main limitations of the Poisson and Matèrn point processes classically used to model emitters location in wireless networks. If the Poisson model is adapted to non-CSMA/CA networks, it appears to be inaccurate in the context of CSMA/CA networks as it does not consider any dependancy between the different transmitters location. The result is an inappropriate interference distribution except for sparse networks. The Matèrn point process, for which we have presented some analytical results, leads to a more realistic model but still suffers from unexpected properties such as an underestimation of concomitant active transmitters and interference level. In consequence, we have proposed the use of an alternate point process, the SSI one, which we assert being a valuable and more appropriate model for CSMA/CA networks. Moreover, we have observed that the interference distributions of the Matèrn and SSI models can be accuratly approximated by a log-normal or a normal distributions in the case of dense networks. This approximation provides the opportunity to analytically study and characterize values such as the Signal over Interference and Noise Ratio (SINR) or the Symbol Error Outage (SEO).

A perspective of this work is to extend the interference model to consider other CCA modes. In other words, these models should be extended to handle a global interference level and no more a single signal level when selecting effective transmitters. We have taken a first step in this perspective with the proposition of constructive point processes such as the SSI one and our temporal alternate Matèrn. More studies now remain to be done and point processes to be explored.

7 Appendix

7.1 Proof of Proposition 2

The area of $\Xi_M(n)$ can be written as follows:

$$\begin{aligned}
\mathbb{E}\left[\Xi_M(n)\right] &= \mathbb{E}\left[\sum_{i=1}^{n}\nu\left(B\cap B_{X_i}\right)\mathbb{1}_{X_i\in\Phi_M(n)}\right]-\mathbb{E}\left[\sum_{i,j=1;j>i}^{n}\nu\left(B\cap B_{X_i}\cap B_{X_j}\right)\mathbb{1}_{(X_i,X_j)\in\Phi_M(n)}\right]\\
&+ \mathbb{E}\left[\sum_{i,j,k=1;k>j>i}^{n}\nu\left(B\cap B_{X_i}\cap B_{X_j}\cap B_{X_k}\right)\mathbb{1}_{(X_i,X_j,X_k)\in\Phi_M(n)}\right]\\
&- \mathbb{E}\left[\sum_{i,j,k,l=1;l>k>j>i}^{n}\nu\left(B\cap B_{X_i}\cap B_{X_j}\cap B_{X_k}\cap B_{X_l}\right)\mathbb{1}_{(X_i,X_j,X_k,X_l)\in\Phi_M(n)}\right]\\
&+ \mathbb{E}\left[\sum_{i,j,k,l,m=1;m>l>k>j>i}^{n}\nu\left(B\cap B_{X_i}\cap B_{X_j}\cap B_{X_k}\cap B_{X_l}\cap B_{X_m}\right)\mathbb{1}_{(X_i,X_j,X_k,X_l,X_m)\in\Phi_M(n)}\right]
\end{aligned}$$

It corresponds to the classical way to compute the area of the union of several balls. In our case, the number of intersections is finite. Indeed, if we consider a point of the plane, this points cannot be covered with a positive probability by more than five balls of radius r and given that the centers of the balls are distant of at least r from each others. The last three terms of the equality above correpond to the functions K_3, K_4 and K_5 of Proposition 2. We compute now each term of the equality. We get for the first term:

$$\begin{aligned}
\mathbb{E}\left[\sum_{i=1}^{n}\nu\left(B\cap B_{X_i}\right)\mathbb{1}_{X_i\in\Phi_M(n)}\right] &= \frac{1}{\pi R^2}\int_B\sum_{i=1}^{n}\nu\left(B\cap B_x\right)\left(\frac{\nu(B\setminus B_x)}{\pi R^2}\right)^{i-1}dx\\
&= \int_B\frac{1}{\pi R^2-\nu(B\setminus B_x)}\nu\left(B\cap B_x\right)\left(1-\left(\frac{\nu(B\setminus B_x)}{\pi R^2}\right)^{n}\right)dx
\end{aligned}$$

Suppose that $n\sim\lambda\pi R^2$ and R tends to infinity, so we can take $\pi R^2-\nu(B\setminus B_x)=\nu(B_x)=\pi r^2$ and $\nu(B\cap B_x)=\pi r^2$. Moreover, $\lim_{R\to+\infty}\left(\frac{\nu(B\setminus B_x)}{\pi R^2}\right)^{\lambda\pi R^2}=e^{-\lambda\pi r^2}$.

The limit is then

$$\lim_{R\to+\infty}\frac{\mathbb{E}\left[\sum_{i=1}^{n}\nu\left(B\cap B_{X_i}\right)\mathbb{1}_{X_i\in\Phi_M(n)}\right]}{\pi R^2} = 1-e^{-\lambda\pi r^2}$$

For the second term, we get:

$$\begin{aligned}
&\mathbb{E}\left[\sum_{i,j=1;j>i}^{n}\nu\left(B\cap\left(B_{X_i}\cap B_{X_j}\right)\right)\mathbb{1}_{(X_i,X_j)\in\Phi_M(n)}\right]\\
&= \frac{1}{(\pi R^2)^2}\int_B\int_{B\setminus B_x}\sum_{i=1}^{n-1}\sum_{j=i+1}^{n}\nu\left(B\cap B_x\cap B_y\right)\left(\frac{\nu(B\setminus(B_x\cup B_y))}{\pi R^2}\right)^{i-1}\left(\frac{\nu(B\setminus B_y)}{\pi R^2}\right)^{j-i-1}dydx\\
&= \int_B\int_{(B\cap B(x,2r))\setminus B_x}\frac{\nu(B\cap B_x\cap B_y)}{\pi R^2-\nu(B\setminus B_x)}\left(\frac{1-\left(\frac{\nu(B\setminus(B_x\cup B_y))}{\pi R^2}\right)^{n-1}}{\pi R^2-\nu(B\setminus(B_x\cup B_y))}\right.\\
&- \left.\frac{\left(\frac{\nu(B\setminus B_x)}{\pi R^2}\right)^{n-1}-\left(\frac{\nu(B\setminus(B_x\cup B_y))}{\pi R^2}\right)^{n-1}}{\pi R^2-\pi R^2\frac{\nu(B\setminus B_x\cup B_y)}{\nu(B\setminus B_x)}}\right)dydx
\end{aligned}$$

When R increases, we can neglect the edge effect, and if $n \sim \lambda \pi R^2$, the second integral does not depends on the location of x we get

$$\begin{aligned}
&\mathbb{E}\left[\sum_{i,j=1;j>i}^{n} \nu\left(B \cap (B_{X_i} \cap B_{X_j})\right) \mathbb{1}_{(X_i,X_j)\in\Phi_M(n)}\right] \\
&\sim \pi R^2 \int_{B(O,2r))\setminus B_O} \frac{\nu(B_O \cap B_y)}{\pi r^2} \left(\frac{1 - \left(\frac{\pi R^2 - \nu(B_O \cup B_y)}{\pi R^2}\right)^{n-1}}{\nu(B_x \cup B_y)} \right. \\
&- \left. \frac{\left(\frac{\pi R^2 - \pi r^2}{\pi R^2}\right)^{n-1} - \left(\frac{\pi R^2 - \nu(B_O \cup B_y)}{\pi R^2}\right)^{n-1}}{\pi R^2 - \pi R^2 \frac{\pi R^2 - \nu(B_O \cup B_y)}{\pi R^2 - \pi r^2}} \right) dy
\end{aligned}$$

We get,

$$\begin{aligned}
&\lim_{R\to+\infty} \frac{\mathbb{E}\left[\sum_{i,j=1;j>i}^{n} \nu\left(B \cap (B_{X_i} \cap B_{X_j})\right) \mathbb{1}_{(X_i,X_j)\in\Phi_M(n)}\right]}{\pi R^2} \\
&= \frac{1}{\pi r^2} \int_{B(O,2r))\setminus B_O} \nu(B_O \cap B_y) \left(\frac{1 - e^{-\lambda \nu(B_O \cup B_y)}}{\nu(B_O \cup B_y)} - \frac{e^{-\lambda \pi r^2} - e^{-\lambda \nu(B_O \cup B_y)}}{\nu(B_O \cup B_y) - \pi r^2} \right) dy
\end{aligned}$$

In the rest of the proof, we use, for convenience, the following notations: $a_z = \nu(B_z)$, $a_{yz} = \nu(B_y \cup B_z)$, $a_{Oyz} = \nu(B_O \cup B_y \cup B_z)$, etc. The same arguments as for the limit above lead to:

$$\begin{aligned}
&\lim_{R\to+\infty} \frac{\mathbb{E}\left[\sum_{i,j,k=1;k>j>i}^{n} \nu\left(B \cap B_{X_i} \cap B_{X_j} \cap B_{X_k}\right) \mathbb{1}_{(X_i,X_j,X_k)\in\Phi_M(n)}\right]}{\pi R^2} \\
&= \int_{B(O,2r)\setminus B_O} \int_{((B_O \cap B_y) \oplus B_O)\setminus(B_O \cup B_y)} \frac{\nu(B_O \cap B_y \cap B_z)}{\pi r^2} \left[\frac{1 - e^{-\lambda a_{Oyz}}}{a_{yz} a_{Oyz}} \right. \\
&+ \left. \left(-\frac{1}{a_{yz}} + \frac{1}{a_{yz} - \pi r^2} \right) \frac{e^{-\lambda a_{yz}} - e^{-\lambda a_{Oyz}}}{a_{Oyz} - a_{yz}} - \frac{e^{-\lambda \pi r^2} - e^{-\lambda a_{Oyz}}}{(a_{yz} - \pi r^2)(a_{Oyz} - \pi r^2)} \right] dz dy \\
&= K_3(\lambda, r)
\end{aligned}$$

where $\oplus$ is the Minkowski-addition (see [22] page 5 for a definition).
For the 4^{th} and 5^{th} quantities, we get:

$$\begin{aligned}
&\lim_{R\to+\infty} \frac{\mathbb{E}\left[\sum_{i,j,k,l=1;l>k>j>i}^{n} \nu\left(B \cap B_{X_i} \cap B_{X_j} \cap B_{X_k} \cap B_{X_l}\right) \mathbb{1}_{(X_i,X_j,X_k,X_l)\in\Phi_M(n)}\right]}{\pi R^2} \\
&= \int_{B(O,2r)\setminus B_O} \int_{((B_O \cap B_y) \oplus B_O)\setminus(B_O \cup B_y)} \int_{((B_O \cap B_y \cap B_z) \oplus B_O))\setminus(B_O \cup B_y \cup B_z)} \frac{\nu(B_O \cap B_y \cap B_z \cap B_v)}{\pi r^2} \\
&\quad \times \left[\frac{1}{a_{zv} a_{yzv} a_{Oyzv}} + \left(-\frac{1}{a_{zv} a_{yzv} a_{Oyzv}} - \frac{c_1}{a_{Oyzv} - a_{yzv}} - \frac{c_2}{a_{Oyzv} - a_{zv}} + \frac{c_3}{a_{Oyzv} - \pi r^2} \right) e^{-\lambda a_{Oyzv}} \right. \\
&+ \left. \frac{c_1}{a_{Oyzv} - a_{yzv}} e^{-\lambda a_{yzv}} + \frac{c_2}{a_{Oyzv} - a_{zv}} e^{-\lambda a_{zv}} - \frac{c_3}{a_{Oyzv} - \pi r^2} e^{-\lambda \pi r^2} \right] dv dz dy \\
&= K_4(\lambda, r)
\end{aligned}$$

with

$$\begin{aligned} c_1 &= -\frac{1}{a_{zv}a_{yzv}} - c_2 + c_3 \\ c_2 &= \frac{\pi r^2}{(a_{zv}-\pi r^2)a_{zv}(a_{yzv}-a_{zv})} \\ c_3 &= \frac{1}{(a_{zv}-\pi r^2)(a_{yzv}-\pi r^2)} \end{aligned}$$

$$\begin{aligned} &\lim_{R\to+\infty} \frac{\mathbb{E}\left[\sum_{i,j,k,l,m=1;m>l>k>j>i}^{n} \nu\left(B\cap B_{X_i}\cap B_{X_j}\cap B_{X_k}\cap B_{X_l}\cap B_{X_m}\right)\mathbb{1}_{(X_i,X_j,X_k,X_l,X_m)\in\Phi_M(n)}\right]}{\pi R^2} \\ &= \int_{B(O,2r)\setminus B_O}\int_{((B_O\cap B_y)\oplus B_O)\setminus(B_O\cup B_y)}\int_{((B_O\cap B_y\cap B_z)\oplus B_O))\setminus(B_O\cup B_y\cup B_z)}\int_{((B_O\cap B_y\cap B_z\cap B_v)\oplus B_O))\setminus(B_O\cup B_y\cup B_z\cup B_v)} \\ &\quad \frac{\nu(B_O\cap B_y\cap B_z\cap B_v\cap B_u)}{\pi r^2}\Bigg[\frac{1}{a_{vu}a_{zvu}a_{yzvu}a_{Oyzvu}} + \Bigg(-\frac{1}{a_{vu}a_{zvu}a_{yzvu}a_{Oyzvu}} - \frac{c_0^{'}}{a_{Oyzvu}-a_{yzvu}} \\ &- \frac{c_1^{'}}{(a_{Oyzvu}-a_{zvu})(a_{yzvu}-a_{zvu})} - \frac{c_2^{'}}{(a_{Oyzvu}-a_{vu})(a_{Oyzvu}-a_{vu})} + \frac{c_3^{'}}{(a_{Oyzvu}-\pi r^2)(a_{Oyzvu}-\pi r^2)}\Bigg) \\ &\times\ e^{-\lambda a_{Oyzvu}} + \frac{c_0^{'}}{a_{Oyzvu}-a_{yzvu}}e^{-\lambda a_{yzvu}} + \frac{c_1^{'}}{(a_{Oyzvu}-a_{zvu})(a_{yzvu}-a_{zvu})}e^{-\lambda a_{zvu}} \\ &+ \frac{c_2^{'}}{(a_{yzvu}-a_{vu})(a_{Oyzvu}-a_{vu})}e^{-\lambda a_{vu}} - \frac{c_3^{'}}{(a_{Oyzvu}-\pi r^2)(a_{yzvu}-\pi r^2)}e^{-\lambda\pi r^2}\Bigg]dvdzdy \\ &= K_5(\lambda,r) \end{aligned}$$

with

$$\begin{aligned} c_0^{'} &= -\frac{1}{a_{vu}a_{zvu}a_{yzvu}} - \frac{c_1^{'}}{a_{yzvu}-a_{zvu}} - \frac{c_2^{'}}{a_{yzvu}-a_{vu}} + \frac{c_3^{'}}{a_{yzvu}-\pi r^2} \\ c_1^{'} &= -\frac{1}{a_{vu}a_{zvu}} + c_3^{'} - c_2^{'} \\ c_2^{'} &= \frac{\pi r^2}{(a_{vu}-\pi r^2)a_{vu}(a_{zvu}-a_{vu})} \\ c_3^{'} &= \frac{1}{(a_{vu}-\pi r^2)(a_{zvu}-\pi r^2)} \end{aligned}$$

7.2 Proof of Proposition 3

The mean interference is given by:

$$\begin{aligned} \mathbb{E}\left[I_{\Phi_M(n)}(O)\right] &= \mathbb{E}\left[\sum_{i=1}^{n} l(\|X_i\|)\mathbb{1}_{X_i\in\Phi_M(n)}\right] \\ &= \frac{1}{\pi R^2}\int_B \sum_{i=1}^{n}\left(\frac{\nu(B\setminus B_x)}{\pi R^2}\right)^{i-1} l(\|x\|)dx \\ &= \int_B \frac{1-\left(\frac{\nu(B\setminus B_x)}{\pi R^2}\right)^n}{\pi R^2-\nu(B\setminus B_x)} l\left(\|x\|\right)dx \\ &= 2\pi\int_0^R u\frac{1-\left(\frac{A(u,r,R)-\pi r^2}{\pi R^2}\right)^n}{\pi R^2+\pi r^2-A(u,r,R)}l(u)du \end{aligned}$$

If n is constant and R tends to infinity, $\mathbb{E}[I_{\Phi_M(n)}(O)]$ tends to 0. If $n \sim \lambda\pi R^2$, we get $\left(\frac{\nu(B\setminus B_x)}{\pi R^2}\right)^{\lambda\pi R^2} \rightarrow e^{-\lambda\pi r^2}$ and we can neglect the edge effects: $\pi R^2 - \nu(B \setminus B_x) = \nu(B_x) = \pi r^2$.

We obtain:

$$\lim_{R\rightarrow+\infty} \mathbb{E}\left[I_{\Phi_M(\lambda\pi R^2)}(O)\right] = \frac{1-e^{-\lambda\pi r^2}}{\pi r^2}\int_{\mathbb{R}^2} l\left(\|x\|\right) dx$$

For the special attenuation function $l(u) = min(1, u^{-\alpha})$ with $\alpha > 2$, we get

$$\lim_{R\rightarrow+\infty} \mathbb{E}\left[I_{\Phi_M(\lambda\pi R^2)}(O)\right] = 2\frac{1-e^{-\lambda\pi r^2}}{r^2}\left(\frac{1}{2}+\frac{1}{\alpha-2}\right)$$

The second moment can also be obtained in the same way. By definition of the interference, we get:

$$\mathbb{E}\left[I^2_{\Phi_M(n)}(O)\right] = \mathbb{E}\left[\sum_{i=1}^{n} l\left(\|X_i\|\right)^2 \mathbb{1}_{X_i\in\Phi_M(n)}\right]$$

$$+2\mathbb{E}\left[\sum_{i=1}^{n-1}\sum_{j=i+1}^{n} l\left(\|X_i\|\right) l\left(\|X_j\|\right) \mathbb{1}_{X_i\in\Phi_M(n)} \mathbb{1}_{X_j\in\Phi_M(n)}\right]$$

For the first term on the right hand side of the equality, the computation is the same as the mean, we get

$$\mathbb{E}\left[\sum_{i=1}^{n} l\left(\|X_i\|\right)^2 \mathbb{1}_{X_i\in\Phi_M(n)}\right] = \int_B \frac{1-\left(\frac{\nu(B\setminus B_x)}{\pi R^2}\right)^n}{\pi R^2 - \nu(B\setminus B_x)} l\left(\|x\|\right)^2 dx \tag{8}$$

For the second term, we get

$$\begin{aligned}
&\mathbb{E}\left[\sum_{i=1}^{n-1}\sum_{j=i+1}^{n} l\left(\|X_i\|\right) l\left(\|X_j\|\right) \mathbb{1}_{X_i\in\Phi_M(n)} \mathbb{1}_{X_j\in\Phi_M(n)}\right] \\
&= \frac{1}{(\pi R^2)^2}\int_B\int_{B\setminus B_x} \sum_{i=1}^{n-1}\sum_{j=i+1}^{n} \left(\frac{\nu(B\setminus B_x\cup B_y)}{\pi R^2}\right)^{i-1} \\
&\quad \left(\frac{\nu(B\setminus B_y)}{\pi R^2}\right)^{j-i-1} l(\|x\|)l(\|y\|)dydx \\
&= \int_B\int_{B\setminus B_x} \frac{1}{\pi R^2 - \nu(B\setminus B_x\cup B_y)}\Big[\frac{1-\left(\frac{\nu(B\setminus B_x\cup B_y)}{\pi R^2}\right)^{n-1}}{\pi R^2 - \nu(B\setminus B_x\cup B_y)} \\
&\quad -\frac{\left(\frac{\nu(B\setminus B_y)}{\pi R^2}\right)^{n-1} - \left(\frac{\nu(B\setminus B_x\cup B_y)}{\pi R^2}\right)^{n-1}}{\pi R^2\left(1-\frac{\nu(B\setminus B_x\cup B_y)}{\nu(B\setminus B_y)}\right)}\Big] l(\|x\|)l(\|y\|)dydx
\end{aligned} \tag{9}$$

When $R \rightarrow +\infty$ and $n \sim \lambda\pi R^2$, we can neglect the edge effects, thus consider that $\pi R^2 - \nu(B \setminus B_x \cup B_y) = \nu(B_x \cup B_y)$ and $\pi R^2 - \pi R^2\frac{\nu(B\setminus B_x\cup B_y)}{\nu(B\setminus B_y)} = \nu(B_x\cup B_y) - \nu(B_y) = \nu(B_x\cup B_y) - \pi r^2$.

Moreover,

$$\lim_{R\rightarrow+\infty}\left(\frac{\nu(B\setminus B_y)}{\pi R^2}\right)^{\lambda\pi R^2-1} = e^{-\lambda\pi r^2}$$

and

$$\lim_{R\rightarrow+\infty}\left(\frac{\nu(B\setminus B_x\cup B_y)}{\pi R^2}\right)^{\lambda\pi R^2} = e^{-\lambda\nu(B_x\cup B_y)}$$

So, if R tends to infinity and $n \sim \lambda\pi R^2$, equations 8 and 9 lead to

$$\lim_{R\to+\infty} \mathbb{E}\left[I^2_{\Phi_M(n)}(O)\right] = \frac{1-e^{-\lambda\pi R^2}}{\pi r^2}\int_{I\!R^2} l\left(\|x\|\right)^2 dx$$

$$+\frac{2}{\pi r^2}\int_{I\!R^2}\int_{I\!R^2\setminus B_x}\left[\frac{1-e^{-\lambda\nu(B_x\cup B_y)}}{\nu(B_x\cup B_y)} - \frac{e^{-\lambda\pi r^2}-e^{-\lambda\nu(B_x\cup B_y)}}{\nu(B_x\cup B_y)-\pi r^2}\right] l\left(\|x\|\right) l\left(\|y\|\right) dydx$$

References

[1] F. Baccelli, B. Błaszczyszyn, and P. Mühlethaler. An aloha protocol for multihop mobile wireless networks. *IEEE Transactions on Information Theory*, 52(2):421–436, 2006.

[2] C. Bettstetter, C. Hartmann, and C. Moser. How does randomized beamforming improve the connectivity of ad hoc networks. In *International Conference on Communications (ICC)*, pages 3380–85, Seoul, Korea, May 2005. IEEE.

[3] T.G. Cheng, Y.-C.; Robertazzi. A new spatial point process for multihop radio network modeling. In *SUPERCOMM/ICC*, 1990.

[4] R. Cook. Stochastic sampling in computer graphics. *ACM Transactions on Graphics*, 5(1):51–72, 1986.

[5] O. Dousse, F. Baccelli, and P. Thiran. Impact of interferences on connectivity in ad hoc networks. *IEEE/ACM Transactions on Networking*, 13(2):425–436, April 2005.

[6] M. Franceschetti, O. Dousse, D. Tse, and P. Thiran. Closing the gap in the capacity of wireless networks via percolation theory. *IEEE Transactions on Information Theory*, 53(3):1009–1018, 2007.

[7] A. Ganesh and G. Torrisi. Large deviations of the interference in a wireless communication model. In *Modeling and Optimization in Mobile, Ad Hoc, and Wireless Networks (WiOpt)*, Limassol, Cyprus,, April 2007.

[8] P. Gupta and P. Kumar. *Critical Power for Asymptotic Connectivity in Wireless Networks*, pages 547–566. (Eds.) Birkhuser, Boston, USA, 1998.

[9] P. Gupta and P. Kumar. Capacity of wireless networks. *IEEE Transactions on Information Theory*, 46(2):388–404, 2000.

[10] P. Hall. *Introduction To the Theory of Coverage Processes*. Wiley, 1988.

[11] R. Hekmat and P. Van Mieghem. Study of connectivity in wireless ad-hoc networks with an improved radio model. In *Modeling and Optimization in Mobile, Ad Hoc, and Wireless Networks (WiOpt)*, Cambridge, UK, 2004.

[12] R. Herczynski. Distribution function for random distribution of spheres. *Nature*, 255:540–541, 1975.

[13] J. Ilow and D. Hatzinakos. Analytic alpha-stable noise modeling in a poisson field of interferers or scatterers. *IEEE Transactions on Signal Processing*, 46(6):1601–1611, June 1998.

[14] W. S. Jodrey and G. M. Tory. Random sequential packing in $I\!R^n$. *Journal of statistical computation and simulation*, 10:87–93, 1980.

[15] B. Matern. Meddelanden fran statens. *Skogsforskningsinstitut*, 2:1–144, 1960.

[16] D. Miorandi. The impact of channel randomness on coverage and connectivity of ad hoc and sensor networks. *IEEE Transactions on Wireless Communications*, 7(3):1062–1072, March 2008.

[17] D. Miorandi and E. Altman. Coverage and connectivity of ad-hoc networks in presence of channel randomness. In *Conference on Computer Communications (INFOCOM)*, volume 1, pages 491–502, Miami, USA, March 2005. IEEE.

[18] H.Q. Nguyen, F. Baccelli, and D. Kofman. A stochastic geometry analysis of dense ieee 802.11 networks. In *Conference on Computer Communications (INFOCOM)*, Anchorage, USA, May 2007. IEEE.

[19] I. Palasti. On some random space filling problem. *Publications of Mathematical Institute of Hungarian Academy of Sciences*, 5(1):353–359, 1960.

[20] R. Sollacher, M. Greiner, and I. Glauche. Impact of interference on the wireless ad-hoc networks capacity and topology. *Wireless Networks*, 12(1):53–61, february 2006.

[21] H. Solomon and H. Weiner. A review of the packing problem. *Communications in Statistics and Theoretical Methods*, 15:2571–2607, 1986.

[22] D. Stoyan, W. Kendall, and J. Mecke. *Stochastic Geometry and Its Applications, 2nd Edition*. John Wiley and Sons Ltd, Chichester, UK, 1996.

[23] D. Tse and P. Viswanath. *Fundamentals of wireless communication*. Cambridge University Press, 2005.

[24] X. Yang and A. P. Petropulu. Co-channel interference modeling and analysis in a poisson field of interferers in wireless communications. *IEEE Transactions on Signal Processing*, 51(1):64–76, January 2003.

[25] J. Yellot. Spectral consequences of photoreceptor sampling in the rhesus retina. *Science*, 221:382–385, 1983.

Centre de recherche INRIA Grenoble – Rhône-Alpes
655, avenue de l'Europe - 38334 Montbonnot Saint-Ismier (France)

Centre de recherche INRIA Bordeaux – Sud Ouest : Domaine Universitaire - 351, cours de la Libération - 33405 Talence Cedex
Centre de recherche INRIA Lille – Nord Europe : Parc Scientifique de la Haute Borne - 40, avenue Halley - 59650 Villeneuve d'Ascq
Centre de recherche INRIA Nancy – Grand Est : LORIA, Technopôle de Nancy-Brabois - Campus scientifique
615, rue du Jardin Botanique - BP 101 - 54602 Villers-lès-Nancy Cedex
Centre de recherche INRIA Paris – Rocquencourt : Domaine de Voluceau - Rocquencourt - BP 105 - 78153 Le Chesnay Cedex
Centre de recherche INRIA Rennes – Bretagne Atlantique : IRISA, Campus universitaire de Beaulieu - 35042 Rennes Cedex
Centre de recherche INRIA Saclay – Île-de-France : Parc Orsay Université - ZAC des Vignes : 4, rue Jacques Monod - 91893 Orsay Cedex
Centre de recherche INRIA Sophia Antipolis – Méditerranée : 2004, route des Lucioles - BP 93 - 06902 Sophia Antipolis Cedex

Éditeur
INRIA - Domaine de Voluceau - Rocquencourt, BP 105 - 78153 Le Chesnay Cedex (France)
http://www.inria.fr
ISSN 0249-6399